Effects of DHEA and DHEAS in Neonatal Hypoxic-Ischemic Brain Injury

Elena Mayer , Ira Winkler , Eva Huber , Martina Urbanek , Ursula Kiechl-Kohlendorfer , Elke Griesmaier , Anna Posod *

Posted Date: 28 October 2024

doi: 10.20944/preprints202410.2113.v1

Keywords: dehydroepiandrosterone; dehydroepiandrosterone sulfate; mouse model; hypoxia-ischemia; neonatal hypoxic-ischemic brain injury; neuroprotection

 doi:10.20944/preprints202410.2113.v1

Article

Effects of DHEA and DHEAS in Neonatal Hypoxic-Ischemic Brain Injury

Elena Mayer, Ira Winkler, Eva Huber, Martina Urbanek, Ursula Kiechl-Kohlendorfer, Elke Griesmaier and Anna Posod *

Department of Pediatrics II (Neonatology), Medical University of Innsbruck, Anichstraße 35, 6020 Innsbruck, Austria

* Correspondence: anna.posod@i-med.ac.at

Abstract: Neonatal brain injury remains a significant issue with limited treatment options. The endogenous neurosteroids dehydroxyepiandrosterone (DHEA) and its sulfate ester (DHEAS) have demonstrated promising therapeutic potential in adult brain injury models due to their neuroprotective mechanisms. This study aimed to analyze the neuroprotective potential of DHEA and DHEAS with a particular interest in anti-oxidative properties in a mouse model of neonatal hypoxic-ischemic brain injury. Using the modified Rice-Vanucci model, brain injury was induced in 7-day-old mouse pups, followed by treatment with various concentrations of DHEA and DHEAS (0.1, 1, and 10 µg/g body weight) via intraperitoneal injection after a 2-hour recovery period. Mice were sacrificed after 24 hours for analysis of somatometry, brain injury, apoptosis, microglial activation, and oxidative stress markers (NOX2, 4-HNE, 8-OHdG), along with the anti-oxidant marker SOD1. No statistically significant effects of the treatments were observed at the tested doses and time points. Although this study did not conclusively demonstrate the anti-oxidative neuroprotective potential of DHEA or DHEAS, neither substance exhibited toxic or harmful effects. Several factors may have contributed to the lack of observable effects, underscoring the need for further refinement in future studies of DHEA(S) and other treatments of neonatal hypoxic-ischemic brain injury.

Keywords: dehydroepiandrosterone; dehydroepiandrosterone sulfate; mouse model; hypoxia-ischemia; neonatal hypoxic-ischemic brain injury; neuroprotection;

1. Introduction

Neonatal encephalopathy is a major cause of mortality and life-long morbidity in newborns [1]. In developed countries, the two most common causes of neonatal brain injury are extremely preterm birth and hypoxic-ischemic encephalopathy (HIE), one of the most severe complications of perinatal asphyxia (PA) [2,3]. PA can be described as a temporary lack of oxygen supply to organ systems following an acute intrapartum hypoxic-ischemic event, which can lead to multi-organ failure in the neonate, potentially affecting the heart, kidneys, lungs, liver and - often most concerning - the brain [4]. Accounting for 23% of neonatal deaths worldwide, PA is the third leading cause of neonatal mortality [5–7].

The majority of hypoxic-ischemic events occur intrapartum [8] and tend to affect different regions of the brain depending on gestational age. While the cortex, thalamus, hippocampus, and basal ganglia are mainly harmed in term infants, white matter is primarily injured in preterm infants [9,10]. The neurological damage results from glucose and oxygen deprivation, which causes a primary energy failure and initiates a cascade of biochemical events leading to cell dysfunction, apoptosis and necrosis of brain cells [10,11]. More specifically, this cascade involves ATP depletion, acidosis, intracellular ion accumulation, neuronal depolarization, uncontrolled release and accumulation of excitatory amino acids, receptor overstimulation leading to massive Ca^{2+} influx and excitotoxicity, mitochondrial dysfunction, production of reactive oxygen species, cell edema, lysis and death [2,12–16]. The etiopathogenesis of neonatal brain injury is complex and still not fully

 doi:10.20944/preprints202410.2113.v1

understood. Current pharmacologic therapies are largely limited to supportive measures, highlighting the need for additional treatment options.

A specific group of substances acting as sigma-1 receptor (σ1R) agonists have shown great potential for the treatment of neonatal brain injury, as their protective effects have been demonstrated in a variety of brain injury models so far [17–22]. One such promising σ1R agonist is the steroid hormone dehydroepiandrosterone (DHEA) and its more stable sulfate ester dehydroepiandrosterone sulfate (DHEAS) [23]. In the brain, endogenous DHEA is involved in neurogenesis, neuroprotection, neuronal growth and survival and has anti-inflammatory, anti-oxidant, anti-glucocorticoid and anti-apoptotic effects [24–30].

Both DHEA and DHEAS have been studied for their beneficial properties in pathological contexts, such as models of neurodegenerative diseases, adult brain injuries and ischemia where they have been shown to protect cells against cell death, neuroinflammation, amyloid beta-protein toxicity, oxidative stress and excitotoxicity in a timing- and dose-dependent manner [26,29–38]. However, both substances have also exhibited pro-apoptotic and neurotoxic properties [34,39]. Research has shown that their mechanisms of action regarding hypoxic-ischemic injury occur primarily through modulation of a number of receptors that are targeted by DHEA, including σ1R, GABA-A receptors, NMDA receptors, NGF receptors and G-protein-coupled receptors [26,28,30,40,41]. However, their neuroprotective potential in neonatal brain injury remains unexplored.

Based on the mechanisms of action and promising potential, we aimed to investigate the therapeutic potential of DHEA and DHEAS in a mouse model of neonatal hypoxic-ischemic brain injury, with a particular interest in their anti-oxidative effects. Due to several factors, including similar levels of the hormone in human and rodent brains, the mouse appears to be a suitable model for DHEA studies in central nervous system function and disease [30].

2. Materials and Methods

All animal experiments were conducted in strict accordance with current European Union legislation (Directive 2010/63/EU, amending Directive 86/609/EEC) and Austrian law. Prior formal approval for the experiments was obtained from our institution's Animal Welfare Body and the Austrian Federal Ministry. All efforts were made to minimize the number of animals used and their suffering. CD-1 mice (Charles River Laboratories, Sulzfeld, Germany) were bred and kept at the Central Laboratory Animal Facility, Medical University of Innsbruck, Austria. Hypoxic-ischemic brain injury was induced by means of a modified version of the Rice-Vannucci model as described previously [42]. In brief, seven-day-old (P7) CD-1 pups were subjected to right common carotid artery ligation under local (lidocaine/prilocaine; AstraZeneca, Wedel, Germany) and general anesthesia (isoflurane in oxygen, 3.0 vol% induction/1.5 vol% maintenance; AbbVie, Vienna, Austria). After a 90-minute recovery period, pups were exposed to a hypoxic environment (8% oxygen in nitrogen) for 20 minutes under normothermic conditions, and subsequently returned to their dams. Following a two-hour recovery period, mouse pups were randomly assigned to one of the following treatment groups: i) control 1x PBS, ii) solvent control 1x PBS + dimethyl sulfoxide (DMSO), iii) DHEA 0.1 µg/g, iv) DHEA 1 µg/g, v) DHEA 10 µg/g, vi) DHEAS 0.1 µg/g, vii) DHEAS 1 µg/g, or viii) DHEAS 10 µg/g body weight. DHEA, DHEAS and DMSO were purchased from Sigma Aldrich (Merck KGaA, Darmstadt, Germany). All mouse pups received a single intraperitoneal (i.p.) injection 2 mm paraumbilically, with an injection volume of 50 µl. They were returned to their dams immediately after treatment until endpoint assessment.

Sex was determined by visual examination of the anogenital region. Body weight was measured on postnatal day 7 (P7) and postnatal day 8 (P8) using calibrated medical precision scales. On P8, mouse pups were sacrificed by decapitation, and brain weight was determined with the same precision scales. Weight gain was calculated as the difference between body weight on P8 and P7, and relative brain weight was determined by dividing brain weight on P8 by body weight on P8. Blood samples were collected in EDTA tubes. Plasma was obtained by centrifugation (1600 x g for 15

 doi:10.20944/preprints202410.2113.v1

min at 4 °C), and pooled based on sex to obtain a minimum volume of 100 µl/sample (3-4 four animals/sample) and stored at −70 °C until further analysis.

Neuropathological Injury Assessment

For histological endpoint determination, brains were harvested, immersion-fixed in 4% formaldehyde for 72–120 hours, paraffin-embedded, and cut into 10-µm-thick coronal sections. Neuropathological injury was assessed in Cresyl Violet-stained sections by a blinded observer using a modified scoring system as described previously [43]. Rating was conducted as follows: 0–4 in cerebral cortex (0, no injury; 1, a few small isolated groups of injured cells; 2, several larger groups of injured cells; 3, moderate confluent infarction; 4, extensive confluent infarction), and 0–3 for mild, moderate, or severe atrophy and neuronal injury/infarction in hippocampus, striatum, and thalamus. A total injury score (0–22) was calculated as the sum of all subratings.

Immunohistochemical Analyses

For immunohistochemical endpoints, paraffin-embedded brain sections were deparaffinized and passed through graded alcohols. Endogenous peroxidases were quenched by incubation with 2% H_2O_2 in methanol for 30 minutes. Heat-induced epitope retrieval was performed with citrate buffer. Unspecific protein blocking was carried out using 5% normal goat serum/ 1% BSA/ 0,1% cold fish skin gelatine/0,5% TritonX-100 in 1x TBS/0,05% Tween 20 for 90 minutes at room temperature. Apoptosis was detected by incubation with rabbit monoclonal anti-cleaved Caspase-3 antibody (1:200, Cell Signaling, Danvers, MA, USA), activated microglia were detected using rabbit anti-ionized calcium-binding adapter molecule 1 (Iba1, 1:1000, Wako, Hong Kong, China). All primary antibodies were diluted in 1%BSA/0,1% cold fish skin gelatine/0,5% TritonX-100 in TBS/0,05% Tween 20 and incubated overnight at 4°C. After rinsing the slides with PBS, the sections were incubated with biotinylated goat anti-rabbit secondary antibody (Jackson Immunoresearch; Szabo Scandic, Vienna, Austria) for 90 minutes at room temperature, followed by incubation with streptavidin-biotin complex (VECTASTAIN Elite ABC Kit, VectorLabs; Szabo Scandic, Vienna, Austria). Enzymatic detection of immunoreactivity was performed by diaminobenzidine substrate kit (Pierce/Fisher Scientific GmbH, Vienna, Austria) for all slides. Staining specificity was ensured by including negative controls in all immunohistochemistry protocols.

The Allen Mouse Brain Coronal Atlas (available from http://brain-map.org) was used as an anatomical reference for brain structures. Quantification of cleaved Caspase-3-positive cells and activated Iba1-positive microglia in the respective regions of interest (ROI) (cortical gray and underlying white matter, hippocampus, thalamus, striatum) of both hemispheres was conducted by a blinded observer at two section planes corresponding to coronal level 72 (bregma -1.755 mm) and coronal level 44 (bregma 1.045 mm). Figure 1 shows representative images of all ROIs. With regard to cleaved Caspase-3, cell counts represent absolute numbers of labeled cells. For microglia quantifications, one representative image from each of the two section planes was chosen for each mouse pup. The area of each ROI was manually delineated and measured by an investigator blinded to lesion and treatment. Activated microglia density (D) was calculated by normalization of the count of amoeboid Iba1-positive cells (C) in the ROI to the measured area (A) of the ROI, also considering the thickness (T) of the section: [D=C/(AxT)]. The analyses were performed using an Olympus IX83 microscope equipped with a DP27 color camera.

 doi:10.20944/preprints202410.2113.v1

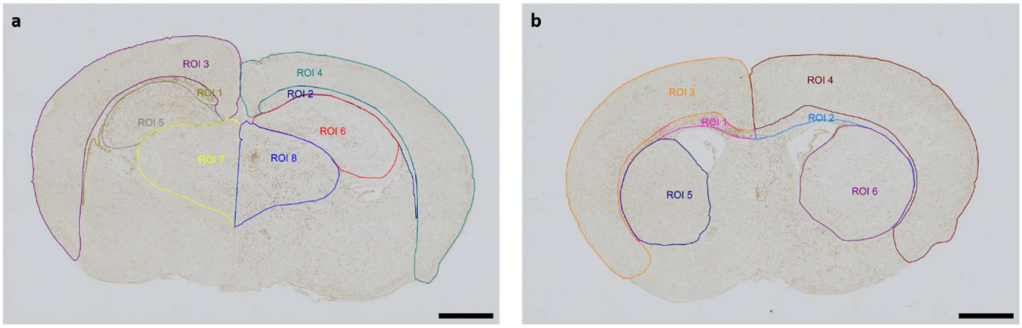

Figure 1. Representative images of Regions of Interest (ROI) were captured in two section planes. Whole-brain visualization was conducted at 40x magnification (scale bars = 1000 µm). The contralateral hemisphere represents the hypoxic-only region, while the ipsilateral hemisphere aligns with the hypoxic-ischemic region. (a) Occipital section plane corresponding to coronal level 72 (bregma -1.755 mm): ROI 1: contralateral white matter, ROI 2: ipsilateral white matter, ROI 3: contralateral cortex, ROI 4: ipsilateral cortex, ROI 5: contralateral hippocampus, ROI 6: ipsilateral hippocampus, ROI 7: contralateral thalamus, ROI 8: ipsilateral thalamus (b) Frontal section plane corresponding to coronal level 44 (bregma 1.045 mm): ROI 1: contralateral white matter, ROI 2: ipsilateral white matter, ROI 3: contralateral cortex, ROI 4: ipsilateral cortex, ROI 5: contralateral striatum, ROI 6: ipsilateral striatum.

Protein Fractionation and Western Blotting

For protein endpoint studies, brains were harvested, snap-frozen in liquid nitrogen and stored at -80°C until further use. Isolation of cytosolic, nuclear and mitochondrial protein fractions was performed according to a modified protocol by Dimauro et al. [44], based on protocols from Cox and Emili [45]. Briefly, brains were homogenized in STM buffer (250 mM sucrose, 50 mM Tris–HCl pH 7.4, 5 mM MgCl2) with protease inhibitors (1x complete EDTA free protease inhibitor cocktail (04693132001, Roche, Vienna, Austria) and 1mM Phenylmethylsulfonyl fluoride (PMSF) (93482, Sigma Aldrich)) and centrifuged at 800 x g for 15 minutes at 4°C producing supernatant containing cytosolic and mitochondrial fractions as well as pellet containing nuclear fraction. Nuclear pellet was centrifuged two more times in STM buffer following resuspension in NET buffer (20 mM HEPES pH 7.9, 1,5 mM MgCl2, 500 mM NaCl, 0,2 mM EDTA pH 8.0, 10% Glycerol, 1% Triton X-100 with protease inhibitors) and kept on ice for 30 minutes. Supernatant with cytosolic and mitochondrial fractions was centrifuged two more times in STM buffer at 11 000 x g for 10 minutes at 4°C. Resulting supernatant containing only cytosolic fractions was transferred to a new tube while mitochondrial pellet was resuspended in ME buffer (20 mM Tris-HCl pH 7.4, 400 mM NaCl, 10% Glycerol, 1% Triton X-100 with protease inhibitors) and kept on ice for 30 minutes. Nuclear and mitochondrial fractions were sonicated three times on ice at high setting for 4-10 seconds and subsequently centrifuged at 9000 x g for 30 minutes at 4°C. Supernatants containing nuclear or mitochondrial fractions were then transferred to a new tube, respectively. Protein quantification of all three fractions was performed using BCA Protein Assay Kit (Fisher Scientific GmbH, Vienna, Austria). Fractionated samples were denatured by heating at 95°C for 5 minutes. 15-20 µg of proteins were separated by SDS-polyacrylamide gel electrophoresis using stain-free gels (4-20% Mini Protean® TGX Stain-Free™ Protein Gels, Biorad, Leipzig, Germany) and transferred to PVDF membranes (Immobilon-PSQ Membrane, Merck Millipore, Molsheim Cedex, France). Membranes were blocked for 1-2 hours in 5% non-fat milk and incubated with primary antibodies over night at 4°C (SOD1 67480-1-Ig, NOX2 19013-1-AP; Proteintech Europe, Manchester, UK). After washing, membranes were incubated with specific horseradish peroxidase-conjugated secondary antibodies (Jackson Immunoresearch; Szabo Scandic, Vienna, Austria) and bands were developed with ECL solution (FastGene Western ECL Kit, Nippon Genetics Europe, Düren, Germany). Quantification of signal density and protein normalization employing β-Actin (clone AC-74, #A5316, Sigma-Aldrich) were conducted using Biorad ImageLab Software 6.1.

 doi:10.20944/preprints202410.2113.v1

ELISA of 4-Hydroxynonenal and 8-Hydroxydesoxyguanosin

Plasma concentrations of 4-Hydroxynonenal (4-HNE) and 8-Hydroxydesoxyguanosin (8-OHdG) were determined by using competitive enzyme-linked immunosorbent assays (ELISAs) according to the manufacturer's instructions (4-HNE: ELSE-EL-0128-96 and 8-OHdG: STRSKT-120-96S, Szabo Scandic, Vienna, Austria). Briefly, pooled mouse plasma was plated in duplicate on a 96-well plate coated with 4-HNE or 8-OHdG respectively. Simultaneously, a biotinylated detection antibody specific for 4-HNE and a horseradish-peroxidase-(HRP-) conjugated detection antibody for 8-OHdG was added to the wells. After incubation, plates were washed several times with washing buffer. For 4-HNE, a HRP-conjugated antibody was added to the plate and again washed after further incubation. Afterwards, Tetramethylbenzidine (TMB) was pipetted to the wells and enzymatic color reaction was developed for 15 to 20 minutes in the dark. Chromogenic reaction was stopped by sulfuric acid and color development was measured at 450 nm using Hidex Sense Microplate Reader (HVD Life Sciences, Vienna, Austria). Sample concentration was determined in ng/mL by employing a calibration curve.

Statistical Analysis

Statistical analysis was performed using SPSS version 29.0 for Windows (IBM Corporation, Armonk, New York) and GraphPad Prism version 10.1.2 for Windows (GraphPad Software, Boston, MA, USA). Data distribution was evaluated by means of histogram analysis as well as Shapiro-Wilk test. If data were normally distributed and no more than two groups were compared at a time, Student's T test was applied. Equality of variances was assessed with Levene's test. Heterogeneity of variances prompted utilization of a modified T test. For analysis of data not belonging to a particular distribution, a Mann-Whitney U test was applied. If more than two groups were compared at a time, overall differences between groups were detected with Analysis of Variance (ANOVA) in case of normal distribution or Kruskal-Wallis test for non-normally distributed data. Post-hoc analysis was conducted by means of Tukey's or Mann-Whitney U test with Bonferroni correction for multiple comparisons. Results were regarded as statistically significant when $p < 0.05$.

3. Results

3.1. Study Population

A total number of 209 mouse pups were subjected to hypoxic-ischemic injury. Of these, 32 (15.3%) died during or shortly after the procedure (n = 27 died prior to i.p. injection, n = 5 died after i.p. injection). The remaining 177 mouse pups were eligible for endpoint assessments. We included 168 mouse pups (male: n = 100, female: n = 68) in the final analysis, 9 mouse pups were excluded due to methodological reasons. Detailed information is provided in Figure 2.

 doi:10.20944/preprints202410.2113.v1

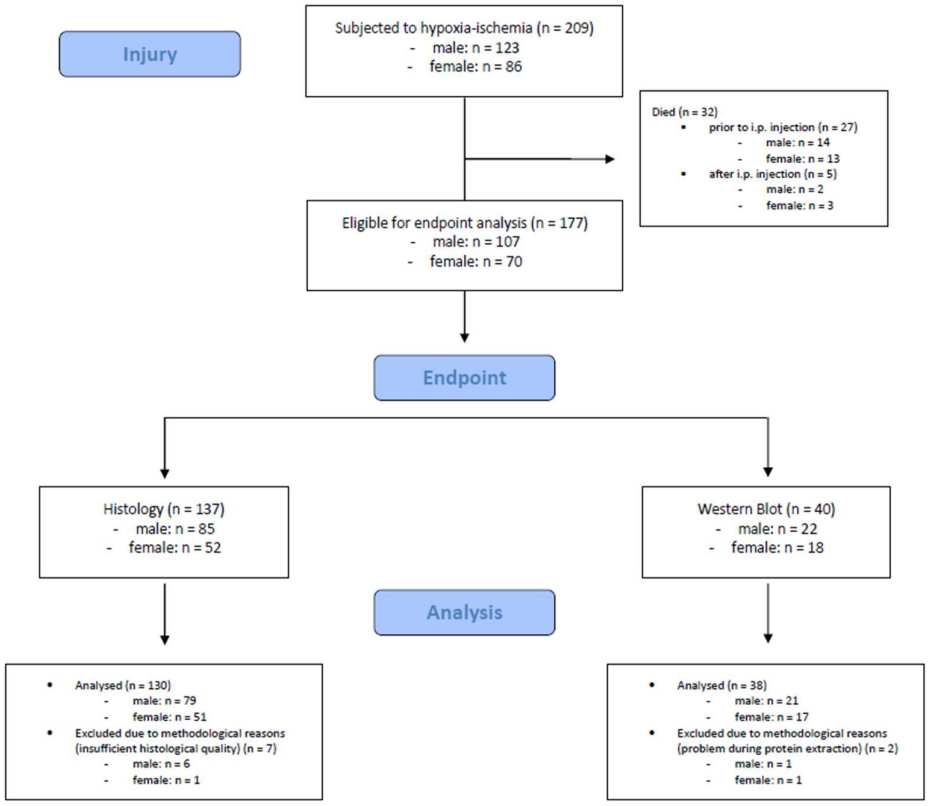

Figure 2. Flow diagram illustrating the experimental workflow and animal cohort distribution.

3.1.1. Somatometry

Somatometric data was obtained from all animals included in endpoint analysis (n = 168). Mean ± standard deviation (SD) body weight on P7 was 4.9 ± 0.5 g; mean ± SD body weight on P8 was 5.3 ± 0.8 g, median (25th; 75th percentile) weight gain was 0.5 (0.2; 0.7) g, median (25th; 75th percentile) brain weight was 0.21 (0.20; 0.22) g, and median (25th; 75th percentile) relative brain weight was 0.040 (0.037; 0.043). Females were lighter on P7 ($p = 0.052$) and P8 ($p = 0.045$), but weight gain and (relative) brain weight did not differ between sexes (all $p > 0.05$). No overall significant differences were detected in any somatometric parameters with regard to treatment (all $p > 0.05$).

3.2. Neuropathological Injury

In neonatal CD-1 mice subjected to hypoxia–ischemia and treated i.p. after insult, a blinded observer assessed neuropathological injury using an established scoring system. No overall statistical differences in neuropathological injury extent were detected in subscores or total injury score (all $p > 0.05$). Details regarding total injury score are provided in Table 1. Representative images of Cresyl Violet stainings for neuropathological injury assessment are shown in Figure 3. No sex-specific differences were observable (all $p > 0.05$).

Table 1. Neuropathological injury assessed in Cresyl Violet-stained sections.

Treatment group	Number of animals, n	Total injury score, median (25th; 75th percentile)	p-value
Control	16	3.5 (1.0; 10.5)	
Solvent control	16	8.3 (0.9; 12.0)	
DHEA 0.1 µg/g bw	15	5.0 (0.5; 13.0)	
DHEA 1 µg/g bw	17	9.5 (1.5; 12.0)	

 doi:10.20944/preprints202410.2113.v1

DHEA 10 µg/g bw	16	5.0 (1.1; 7.9)	
DHEAS 0.1 µg/g bw	16	7.5 (1.3; 12.8)	
DHEAS 1 µg/g bw	17	4.0 (1.3; 11.0)	
DHEAS 10 µg/g bw	17	6.5 (1.5; 12.5)	0.829[1]

Abbreviations: DHEA, dehydroepiandrosterone; *DHEAS*, dehydroepiandrosterone sulfate; *bw*, body weight. [1] Overall statistical differences assessed by Kruskal-Wallis test ($H_{(7)} = 3.561$).

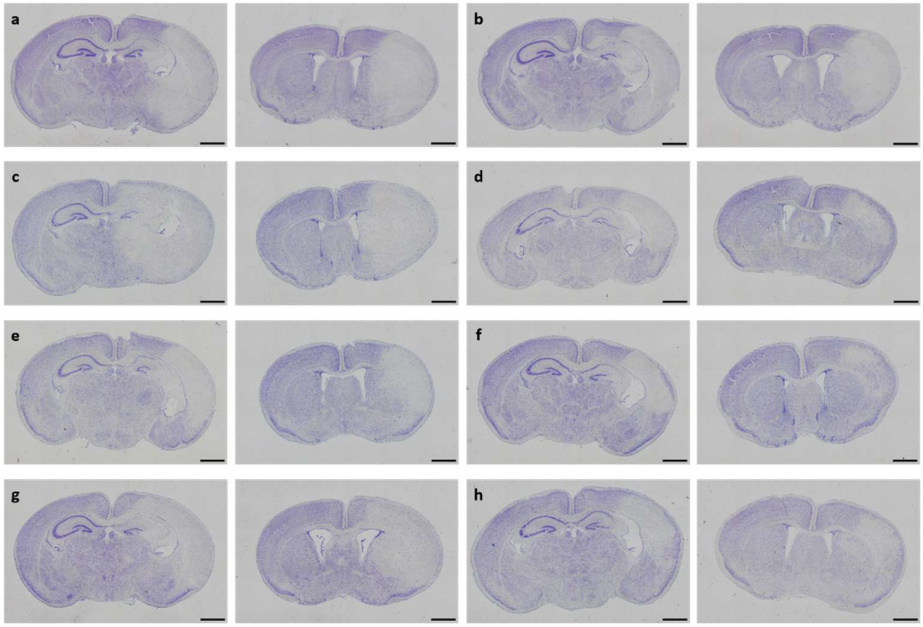

Figure 3. Neuropathological injury assessment. Representative images of Cresyl Violet-stained coronal brain sections displaying hypoxic-ischemic injury in different treatment groups (a-h). Whole-brain visualization was performed using a 40-fold magnification (scale bars = 1000 µm). Two coronal section planes corresponding to coronal level 72 (bregma -1.755 mm, left) and coronal level 44 (bregma 1.045 mm, right), are displayed per brain. Treatment groups are as follows: (**a**) control 1x PBS, (**b**) solvent control 1x PBS+DMSO, (**c**) DHEA 0.1 µg/g bodyweight (bw), (**d**) DHEA 1 µg/g bw, (**e**) DHEA 10 µg/g bw, (**f**) DHEAS 0.1 µg/g bw, (**g**) DHEAS 1 µg/g bw, (**h**) DHEAS 10 µg/g bw.

3.3. Anti-Apoptotic Potential of DHEA and DHEAS

To assess the neuroprotective potential of DHEA and DHEAS against apoptosis, immunohistochemical quantification of activated Caspase-3-positive cells was performed in six mouse pups per treatment group. Detection of activated Caspase-3 is considered a reliable marker for apoptotic or pre-apoptotic cells [46]. Analysis was conducted on two coronal section planes, examining both the contralateral (hypoxic-only) hemisphere and the ipsilateral (hypoxic-ischemic) hemisphere. Representative photomicrographs of activated Caspase-3 immunohistochemistry are shown in Figure 4. No significant overall differences in Caspase-3 activation were detectable. Details are provided in Table 2. No sex-specific differences in Caspase-3 activation were observed in any brain region across all treatment groups (all $p > 0.05$).

 doi:10.20944/preprints202410.2113.v1

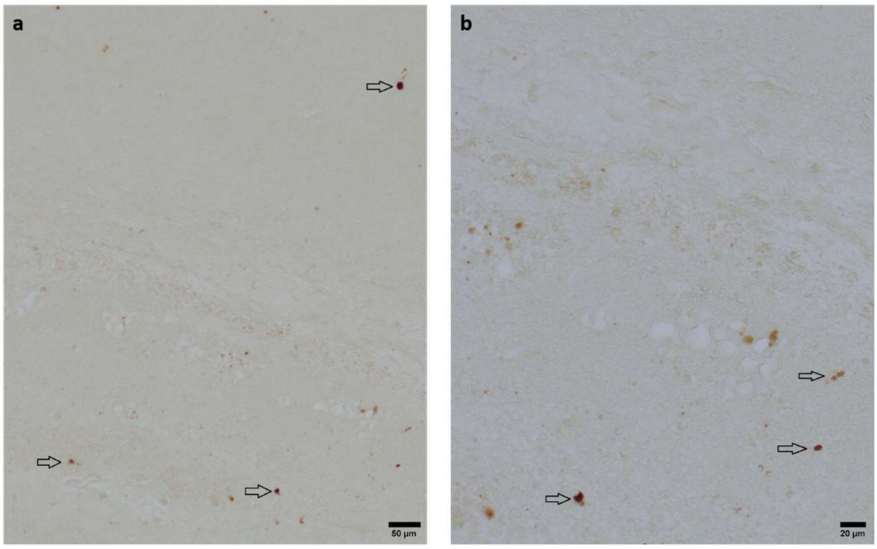

Figure 4. Representative photomicrographs of activated Caspase-3-positive cells in occipital section plane cortex and white matter (coronal level 72, bregma -1.755 mm). Arrows indicate positive cells. Visualization was performed using a 100-fold (scale bar = 50 µm) (**a**) and 200-fold magnification (scale bar = 20 µm) (**b**).

Table 2. Number of activated Caspase-3-positive cells per brain region.

Section plane	Hemisphere	Brain region	Treatment group	Number of positive cells, median (25th; 75th percentile)	p-value
Occipital	Contralateral	White matter			
			Control	11 (4; 12)	
			Solvent control	6 (4; 10)	
			DHEA 0.1 µg/g bw	6 (4; 11)	
			DHEA 1 µg/g bw	13 (11; 16)	
			DHEA 10 µg/g bw	10 (6; 14)	
			DHEAS 0.1 µg/g bw	11 (3; 23)	
			DHEAS 1 µg/g bw	7 (6; 10)	
			DHEAS 10 µg/g bw	8 (6; 11)	0.268[1]
	Ipsilateral	White matter			
			Control	125 (12; 181)	
			Solvent control	16 (4; 162)	
			DHEA 0.1 µg/g bw	19 (11; 111)	
			DHEA 1 µg/g bw	182 (10; 282)	
			DHEA 10 µg/g bw	27 (10; 141)	
			DHEAS 0.1 µg/g bw	121 (7; 248)	

 doi:10.20944/preprints202410.2113.v1

		DHEAS 1 µg/g bw	25 (9; 228)	
		DHEAS 10 µg/g bw	83 (17; 230)	0.836[1]
Contralateral	Cortex			
		Control	16 (13; 25)	
		Solvent control	16 (9; 20)	
		DHEA 0.1 µg/g bw	23 (14; 33)	
		DHEA 1 µg/g bw	24 (13; 32)	
		DHEA 10 µg/g bw	15 (9; 24)	
		DHEAS 0.1 µg/g bw	20 (13; 24)	
		DHEAS 1 µg/g bw	20 (16; 26)	
		DHEAS 10 µg/g bw	19 (15; 23)	0.590[1]
Ipsilateral	Cortex			
		Control	160 (37; 276)	
		Solvent control	37 (10; 202)	
		DHEA 0.1 µg/g bw	39 (25; 107)	
		DHEA 1 µg/g bw	286 (23; 376)	
		DHEA 10 µg/g bw	34 (24; 220)	
		DHEAS 0.1 µg/g bw	158 (18; 446)	
		DHEAS 1 µg/g bw	39 (27; 169)	
		DHEAS 10 µg/g bw	93 (25; 366)	0.901[1]
Contralateral	Hippocampus			
		Control	4 (3; 5)	
		Solvent control	3 (2; 5)	
		DHEA 0.1 µg/g bw	5 (4; 5)	
		DHEA 1 µg/g bw	5 (3; 6)	
		DHEA 10 µg/g bw	4 (2; 6)	
		DHEAS 0.1 µg/g bw	5 (3; 9)	
		DHEAS 1 µg/g bw	4 (4; 6)	
		DHEAS 10 µg/g bw	4 (3; 6)	0.882[1]
Ipsilateral	Hippocampus			
		Control	69 (23; 87)	
		Solvent control	35 (5; 96)	

 doi:10.20944/preprints202410.2113.v1

			DHEA 0.1 µg/g bw	48 (25; 109)	
			DHEA 1 µg/g bw	81 (4; 107)	
			DHEA 10 µg/g bw	41 (8; 115)	
			DHEAS 0.1 µg/g bw	53 (8; 159)	
			DHEAS 1 µg/g bw	51 (7; 112)	
			DHEAS 10 µg/g bw	70 (49; 135)	0.951[1]
	Contralateral	Thalamus			
			Control	6 (5; 15)	
			Solvent control	6 (4; 11)	
			DHEA 0.1 µg/g bw	7 (4; 12)	
			DHEA 1 µg/g bw	6 (5; 10)	
			DHEA 10 µg/g bw	15 (6; 25)	
			DHEAS 0.1 µg/g bw	9 (6; 12)	
			DHEAS 1 µg/g bw	7 (4; 8)	
			DHEAS 10 µg/g bw	7 (4; 16)	0.680[1]
	Ipsilateral	Thalamus			
			Control	43 (15; 113)	
			Solvent control	16 (6; 64)	
			DHEA 0.1 µg/g bw	12 (6; 29)	
			DHEA 1 µg/g bw	35 (8; 65)	
			DHEA 10 µg/g bw	10 (6; 41)	
			DHEAS 0.1 µg/g bw	15 (4; 38)	
			DHEAS 1 µg/g bw	8 (5; 22)	
			DHEAS 10 µg/g bw	23 (10; 39)	0.381[1]
Frontal	Contralateral	White matter			
			Control	6 (4; 10)	
			Solvent control	6 (5; 10)	
			DHEA 0.1 µg/g bw	8 (6; 9)	
			DHEA 1 µg/g bw	11 (7; 14)	
			DHEA 10 µg/g bw	4 (4; 8)	

 doi:10.20944/preprints202410.2113.v1

Ipsilateral	White matter	DHEAS 0.1 µg/g bw	5 (3; 10)	
		DHEAS 1 µg/g bw	5 (4; 18)	
		DHEAS 10 µg/g bw	8 (5; 13)	0.494[1]
		Control	22 (9; 52)	
		Solvent control	9 (4; 30)	
		DHEA 0.1 µg/g bw	8 (7; 27)	
		DHEA 1 µg/g bw	35 (12; 62)	
		DHEA 10 µg/g bw	6 (4; 17)	
		DHEAS 0.1 µg/g bw	16 (3; 67)	
		DHEAS 1 µg/g bw	7 (2; 30)	
		DHEAS 10 µg/g bw	14 (6; 29)	0.409[1]
Contralateral	Cortex			
		Control	16 (13; 30)	
		Solvent control	17 (9; 20)	
		DHEA 0.1 µg/g bw	23 (17; 32)	
		DHEA 1 µg/g bw	16 (10; 22)	
		DHEA 10 µg/g bw	15 (10; 17)	
		DHEAS 0.1 µg/g bw	15 (11; 22)	
		DHEAS 1 µg/g bw	16 (14; 18)	
		DHEAS 10 µg/g bw	14 (9; 24)	0.468[1]
Ipsilateral	Cortex			
		Control	89 (24; 231)	
		Solvent control	26 (9; 107)	
		DHEA 0.1 µg/g bw	23 (16; 93)	
		DHEA 1 µg/g bw	145 (24; 204)	
		DHEA 10 µg/g bw	13 (9; 68)	
		DHEAS 0.1 µg/g bw	54 (9; 184)	
		DHEAS 1 µg/g bw	21 (15; 85)	
		DHEAS 10 µg/g bw	59 (24; 92)	0.351[1]
Contralateral	Striatum			

 doi:10.20944/preprints202410.2113.v1

		Control	6 (4; 10)	
		Solvent control	6 (3; 8)	
		DHEA 0.1 µg/g bw	9 (7; 13)	
		DHEA 1 µg/g bw	9 (4; 11)	
		DHEA 10 µg/g bw	8 (6; 11)	
		DHEAS 0.1 µg/g bw	6 (4; 9)	
		DHEAS 1 µg/g bw	5 (4; 9)	
		DHEAS 10 µg/g bw	5 (4; 6)	0.305[1]
Ipsilateral	Striatum			
		Control	92 (8; 198)	
		Solvent control	13 (5; 104)	
		DHEA 0.1 µg/g bw	12 (9; 117)	
		DHEA 1 µg/g bw	130 (15; 288)	
		DHEA 10 µg/g bw	10 (4; 15)	
		DHEAS 0.1 µg/g bw	15 (4; 72)	
		DHEAS 1 µg/g bw	9 (5; 85)	
		DHEAS 10 µg/g bw	16 (10; 69)	0.296[1]

Occipital section plane corresponds to coronal level 72 (bregma -1.755 mm), frontal section plane corresponds to coronal level 44 (bregma 1.045 mm). *Abbreviations: DHEA*, dehydroepiandrosterone; *DHEAS*, dehydroepiandrosterone sulfate; *bw*, body weight. [1] Overall statistical differences assessed by Kruskal-Wallis test.

3.4. Microglial Cell Activation

To assess microglial cell activation, immunohistochemical quantification of activated Iba1-positive microglia was performed in six mouse pups per treatment group. The activation status of each cell was determined based on morphology. Density of Iba1-positive cells was calculated for each ROI to account for differences in size of brain regions. Analysis was conducted on two coronal section planes, examining both the contralateral (hypoxic-only) hemisphere and the ipsilateral (hypoxic-ischemic) hemisphere. Representative photomicrographs of activated Iba1-positive microglial cells are shown in Figure 5. Although brain regions exposed to hypoxia-ischemia generally showed stronger glial activation compared to hypoxic-only regions, microglial activation did not differ significantly between treatment groups (all $p > 0.05$) (Figure 6). No sex-specific differences in activated microglia density were observed in any brain region across all treatment groups (all $p > 0.05$).

 doi:10.20944/preprints202410.2113.v1

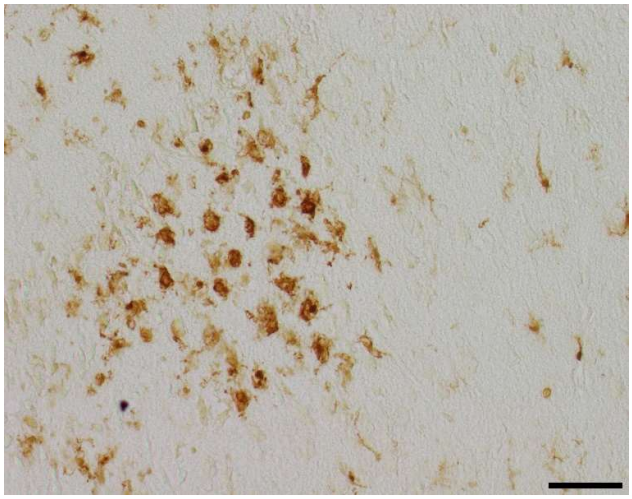

Figure 5. Representative photomicrographs of activated Iba1-positive microglial cells in occipital section plane cortex (coronal level 72, bregma -1.755 mm). Visualization was performed using a 200-fold (scale bar = 50 μm) magnification.

 doi:10.20944/preprints202410.2113.v1

a

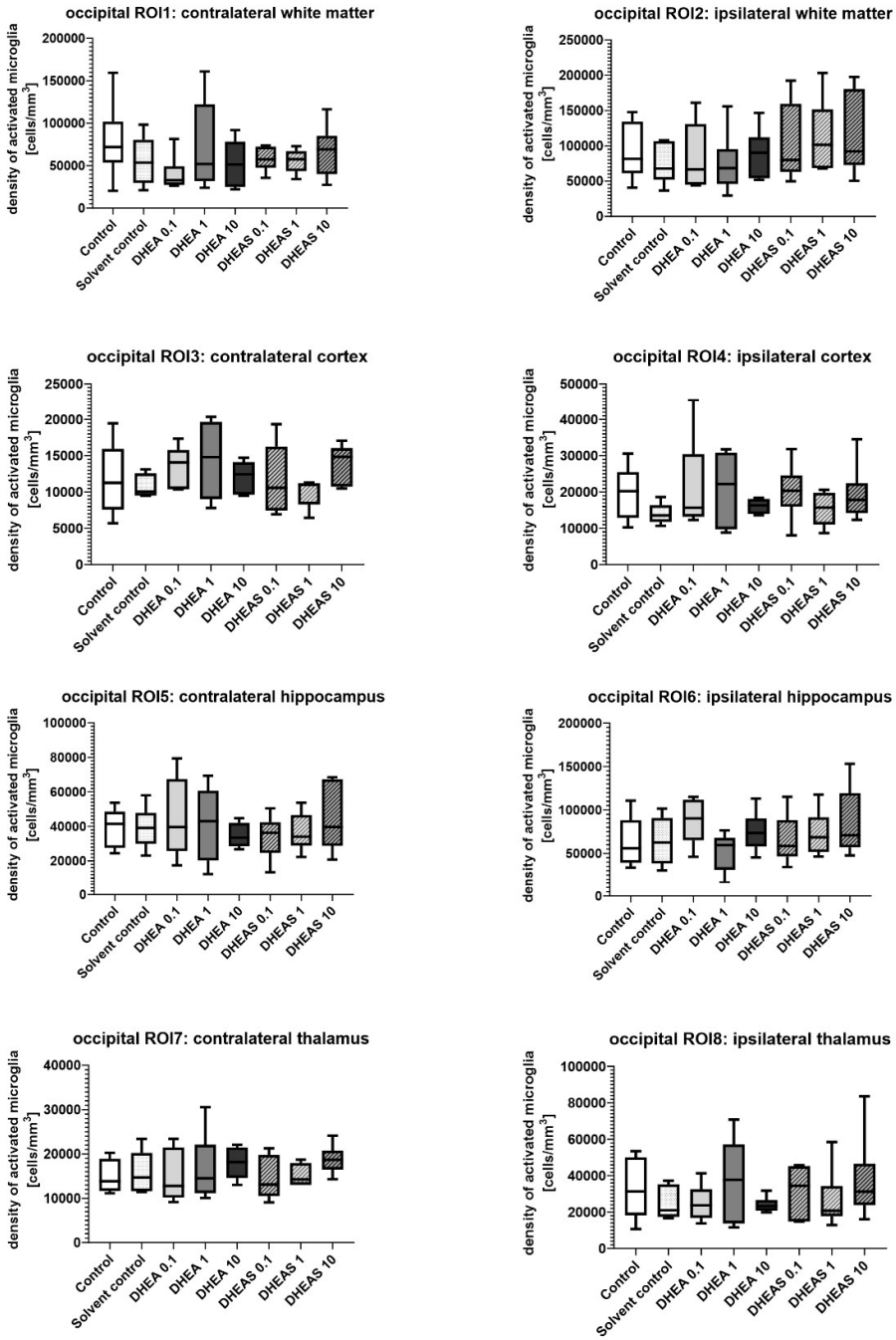

 doi:10.20944/preprints202410.2113.v1

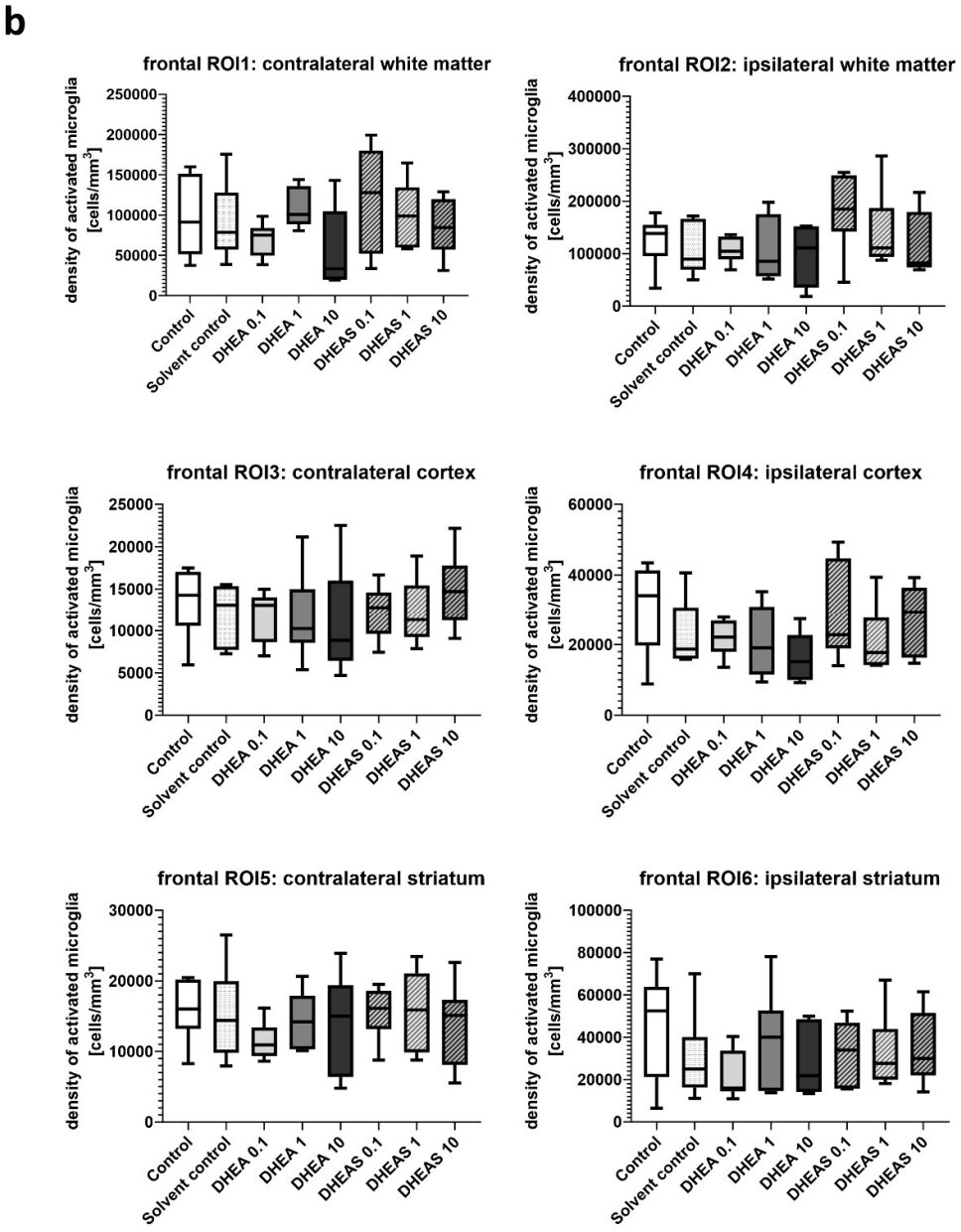

Figure 6. Microglial activation in different brain regions in the occipital (**a**) and frontal (**b**) section plane. Occipital section plane (**a**) corresponds to coronal level 72 (bregma -1.755 mm). Frontal section plane (**b**) corresponds to coronal level 44 (bregma 1.045 mm). Numbers in the different treatment groups indicate concentrations in µg/g bodyweight. Center lines in the boxes represent medians, box edges mark 1st and 3rd quartiles, and whiskers indicate 10th and 90th percentiles. No overall significant differences in microglial cell activation in the analyzed brain regions were detected (Kruskal-Wallis test, all $p > 0.05$). Animals per group: n = 6.

3.5. Anti-Oxidative Potential of DHEA and DHEAS

3.5.1. Upstream Markers of Oxidative Stress—Western Blot

To evaluate the anti-oxidative potential of DHEA and DHEAS, we analyzed two upstream markers of oxidative stress, SOD1 and NOX2, in pooled protein extracts of either brain hemisphere

 doi:10.20944/preprints202410.2113.v1

via Western Blot. SOD1 constitutes a front-line defense mechanism against oxidative stress acting as an anti-oxidant, while NOX2 is a major source of oxidative stress [47,48]. Since SOD1 and NOX2 are expected to be primarily present in cytosolic protein fractions, only the results of this fraction are presented. Although a trend towards increased SOD1 expression could be observed in DHEA(S)-treated animals, no statistically significant differences in SOD1 expression were detected in any protein fraction of either hemisphere across all treatment groups (all $p > 0.05$) (Figure 7). Similarly, no significant effects of the treatments on NOX2 expression were observed (all $p > 0.05$) (Figure 8). Sex-specific differences were not assessed due to limited case numbers.

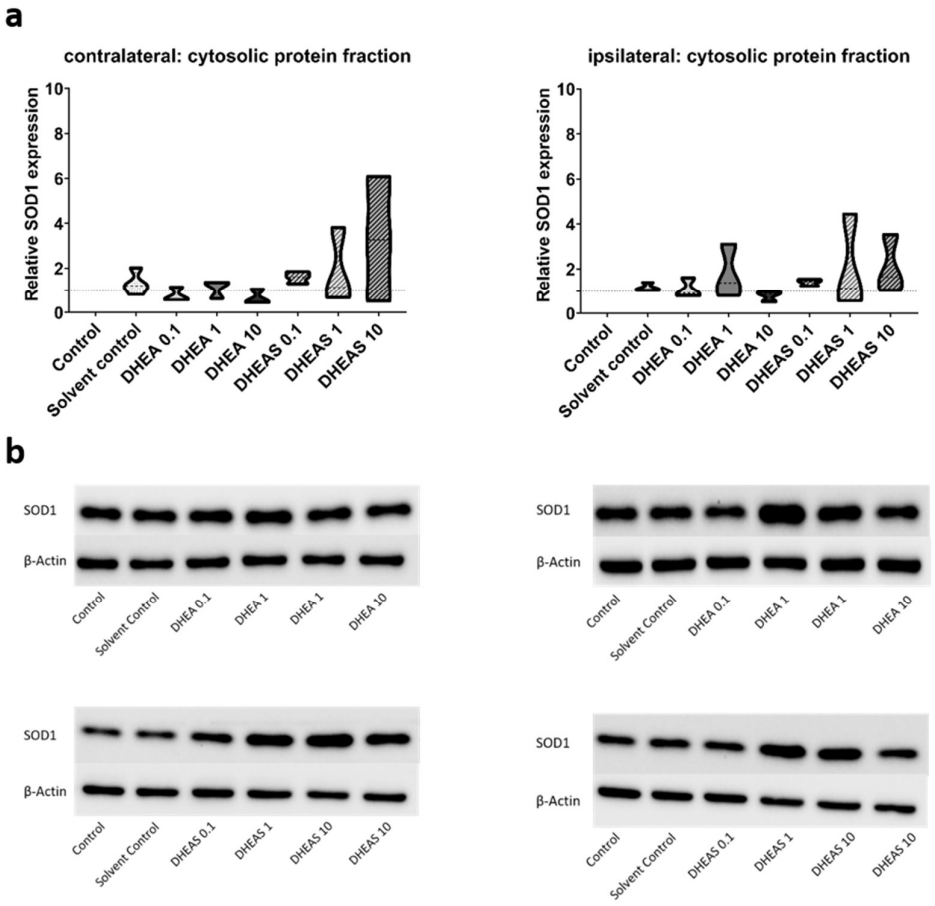

Figure 7. Relative SOD1 expression across treatment groups. Numbers in the different treatment groups indicate concentrations in µg/g bodyweight. (**a**) Truncated violin plots depict the distribution of relative SOD1 expression levels in different treatment groups in cytosolic protein fractions of the contralateral and the ipsilateral hemisphere, with the control group set to 1 (dotted line). The width of the violins corresponds to the frequency of observations at each expression level. The extreme tails of the distributions were truncated to highlight the central portion of the data, emphasizing the median (dashed lines), the interquartile range (black lines), and the overall shape of the distribution. The control group serves as the baseline for comparison, and its distribution is centered around 1. Number of pooled samples per group: n = 3-4. (**b**) Exemplary Western Blots showing SOD1 reactivity in different treatment groups in the contralateral (left) and ipsilateral hemisphere (right). β-Actin served as a loading control.

 doi:10.20944/preprints202410.2113.v1

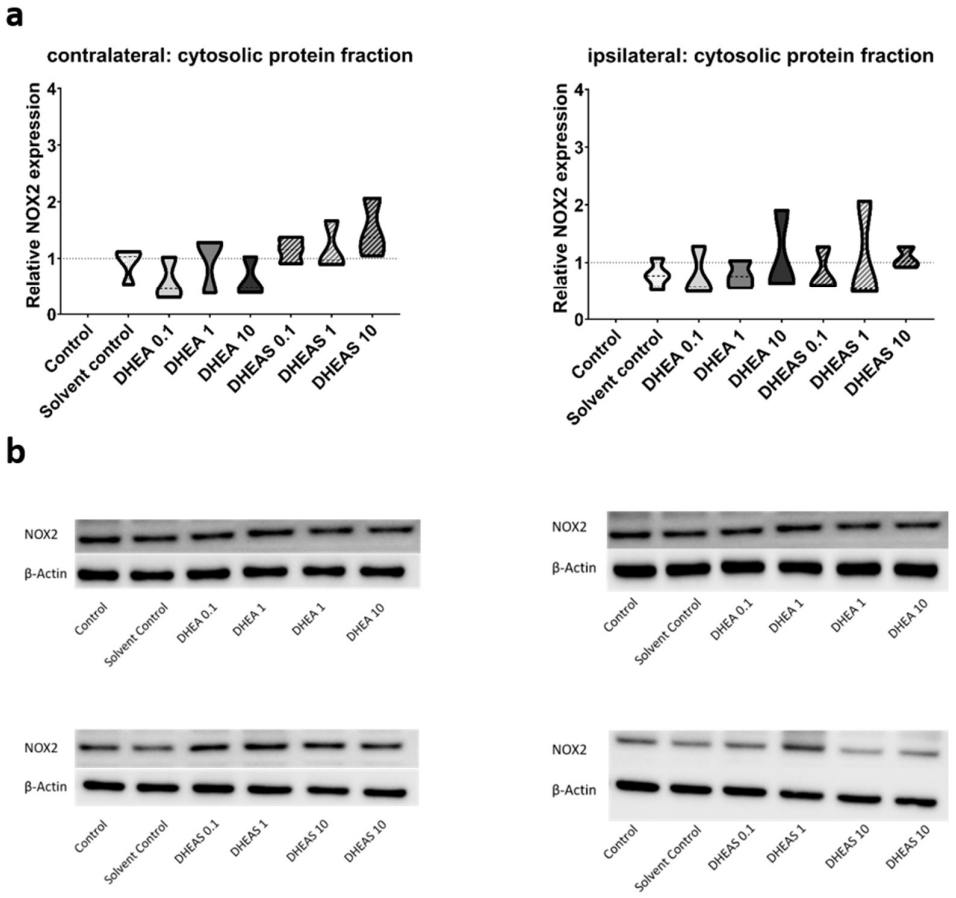

Figure 8. Relative NOX2 expression across treatment groups. Numbers in the different treatment groups indicate concentrations in µg/g bodyweight. (**a**) Truncated violin plots depict the distribution of relative NOX2 expression levels in different treatment groups in cytosolic protein fractions of the contralateral and the ipsilateral hemisphere, with the control group set to 1 (dotted line). The width of the violins corresponds to the frequency of observations at each expression level. The extreme tails of the distributions were truncated to highlight the central portion of the data, emphasizing the median (dashed lines), the interquartile range (black lines), and the overall shape of the distribution. The control group serves as the baseline for comparison, and its distribution is centered around 1. Number of pooled samples per group: n = 3-4. (**b**) Exemplary Western Blots showing NOX2 reactivity in different treatment groups in the contralateral (left) and ipsilateral hemisphere (right). β-Actin served as a loading control.

3.5.2. Downstream Markers of Oxidative Stress—ELISA

To assess oxidative stress also downstream, we quantified 4-HNE and 8-OHdG in pooled plasma samples using ELISAs. 4-HNE is considered one of the major mediators of oxidative stress and an important downstream marker of lipid peroxidation [49]. The nucleotide 8-OHdG is one of the major DNA damage types induced by oxidative stress and therefore considered a pivotal marker of oxidative DNA damage [50]. Plasma concentrations of both tested oxidation markers showed no overall significant differences across treatment groups (all $p > 0.05$) (Figure 9). In addition, no sex-specific differences were detectable (all $p > 0.05$).

 doi:10.20944/preprints202410.2113.v1

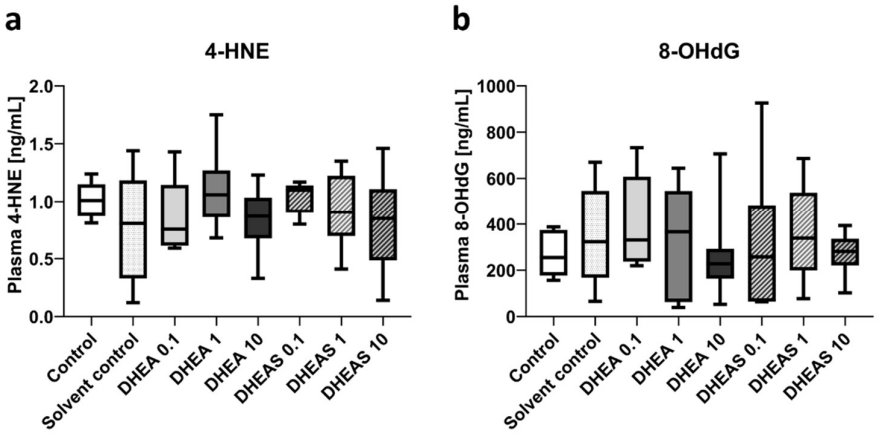

Figure 9. Plasma concentrations of oxidative stress markers 4-HNE **(a)** and 8-OHdG **(b)**. Numbers in the different treatment groups indicate concentrations in μg/g bodyweight. Center lines in the boxes represent medians, box edges mark 1st and 3rd quartiles, and whiskers indicate 10th and 90th percentiles. (**a**) No overall significant differences in 4-HNE plasma concentrations were detected. Number of pooled samples per group: n = 5-6. (**b**) No overall significant differences in 8-OHdG plasma levels were detected. Number of pooled samples per group: n = 6-8.

4. Discussion

Hypoxic-ischemic brain injury continues to be a major cause of mortality and morbidity among neonates worldwide. Despite this, little progress has been made in pharmacologic treatment options over the past few decades, with most being limited to supportive measures. This highlights the importance of finding additional therapeutic agents for treating neonatal HIE.

In previous research, both DHEA and DHEAS have shown neuroprotective, anti-apoptotic and anti-inflammatory properties in adult models of brain injury, overall demonstrating great therapeutic potential [31–33,35–37,40]. This study aimed to evaluate the neuroprotective potential of DHEA and DHEAS, specifically focusing on their anti-oxidative effects in a neonatal model of hypoxic-ischemic brain injury.

In this study, the neuroprotective and anti-oxidative properties of DHEA and DHEAS were explored at various doses (0.1 μg, 1 μg, or 10 μg per g body weight), with no significant reduction in injury scores, apoptosis, microglial activation or oxidative stress markers across the groups. However, we demonstrated that DHEA and DHEAS have no negative impact on injured brains. The absence of observable therapeutic benefits in reducing oxidative stress and neuronal damage might stem from a number of factors including the dosing strategy. While neurosteroids like DHEA and DHEAS often exhibit dose-dependent effects and the beneficial effects of both substances have been shown to be highly timing- and dosage-dependent, there is no consensus regarding the optimal conditions for neurosteroid use in similar models [30–32,34–38]. Previous studies suggest an inverted U-shaped dose-response curve for DHEA and DHEAS, where moderate concentrations yield the best results, while excessively high or low doses can be either ineffective or even neurotoxic [30]. Importantly, much of this research has been conducted in adult rodents, where higher doses (ranging from 20 to 100 mg/kg) were found to be effective [34,36,38,51,52]. This study used lower doses due to solubility limitations of DHEA(S) in PBS and concerns regarding the potentially harmful effects of the solvent DMSO [53]. Consequently, the administered doses may not have achieved the concentrations necessary for eliciting a neuroprotective anti-oxidative response.

Secondly, the route of administration and timing are crucial factors in neuroprotective studies. Here, DHEA and DHEAS were administered via intraperitoneal injection after a two-hour recovery period post-injury. While intraperitoneal administration is practical for neonatal models, it may limit the drug's ability to cross the blood-brain barrier, particularly for DHEAS, which is more hydrophilic

 doi:10.20944/preprints202410.2113.v1

than DHEA. Higher dosages or a different route of administration may enhance the permeability and effectiveness of DHEAS.

Additionally, timing of treatment plays a pivotal role in neuroprotective efficacy. In this study, the compounds were administered during the latent phase of HIE, which is considered optimal for interventions aimed at preventing secondary injury. However, there is no consensus regarding optimal timing of DHEA(S) treatment in the literature with some studies demonstrating significant protective effects when either administered before, during or within minutes after injury, while others employed continuous or repeated dosing strategies post-injury [31,35,36,51,52,54–56]. Contrary to this, Li and colleagues reported neurotoxic effects when administered too early and showed that treatment 3 to 48 hours after injury yielded the best outcome [34]. This lack of consensus highlights the need for future studies investigating whether early, delayed or repeated administration of DHEA(S) can improve brain damage in neonates.

Another limitation in the present study is the early endpoint analysis conducted 24 hours after the hypoxic-ischemic event. While this timeframe captures early injury markers, it may not fully reflect the long-term neuroprotective effects or the extent of oxidative damage mitigated by DHEA(S). Since other studies involving longer observation periods (up to several weeks) have shown that delayed administration of DHEA(S) can lead to improvements in cognitive and behavioral outcomes, we cannot rule out that our limited 24-hour window may have overlooked subtle anti-oxidative and neuroprotective benefits that could become apparent in a more extended timeframe [34,36,38,51,52,55].

One major factor likely contributing to the inconclusive results is the inherent variability in the experimental model used in this study. The modified Rice-Vannucci model is known for a certain degree of variability in resulting brain injuries and despite efforts to standardize conditions, variations in injury severity and treatment responses were still observed among the individual pups, potentially confounding the outcomes. This variability is consistent with the challenges of studying neuroprotective agents in neonatal models, where factors such as the sex of the pups, differences in brain development, and individual susceptibility to oxidative stress play significant roles, further complicating detection of distinct effects.

Moreover, the study's small sample size may have limited the statistical power to detect subtle anti-oxidative effects, particularly given the inherent variability within the model. More samples in each analyzed group could have possibly revealed more nuanced effects. This, for example, is indicated by the results of SOD1. A trend towards increased SOD1 expression could be observed in DHEA(S)-treated animals, but due to the small sample size of n = 3 for these groups, the results were not significant. In some instances, samples from mice receiving the same treatment were also pooled due to limited protein extraction quantities, potentially diluting individual differences and masking potential anti-oxidative effects of DHEA and DHEAS.

Finally, the unexpected absence of neuroprotective effects in this study may also be attributed to the differences between the maturing brain of a newborn and the adult brain. In recent years, research has shown that the neonatal brain is not just a smaller version of the adult brain, and therefore the pathophysiology as well as the therapeutic approach to its injury may differ greatly [57].

5. Conclusions

In conclusion, this study did not observe significant anti-oxidative neuroprotective effects of DHEA or DHEAS at the tested doses and timing in a neonatal hypoxic-ischemic brain injury model. However, several factors, including the route of administration, dosing strategies, timing of intervention, and early endpoint analysis, may have contributed to the lack of observable effects. Future research should focus on optimizing these parameters to better evaluate the therapeutic potential of DHEA and DHEAS.

Given their well-documented anti-oxidative properties in adult models, these neurosteroids remain promising candidates for neonatal neuroprotection. Further studies should explore higher or repeated doses, alternative administration routes, and extended observation periods to fully capture the long-term benefits of DHEA(S). Additionally, future investigations should account for sex-

 doi:10.20944/preprints202410.2113.v1

specific responses and aim to identify biomarkers that can predict individual treatment efficacy in neonatal populations.

Although this study did not conclusively demonstrate the anti-oxidative neuroprotective potential of DHEA or DHEAS, it found no detrimental effects. It also highlights critical areas for refinement in future neuroprotection studies targeting neonatal hypoxic-ischemic brain injury.

Author Contributions: Conceptualization, Elke Griesmaier and Anna Posod; Data curation, Elena Mayer, Eva Huber, Martina Urbanek and Anna Posod; Formal analysis, Elena Mayer and Anna Posod; Funding acquisition, Anna Posod; Investigation, Elena Mayer and Anna Posod; Methodology, Elena Mayer, Eva Huber and Martina Urbanek; Project administration, Eva Huber and Anna Posod; Resources, Ursula Kiechl-Kohlendorfer and Elke Griesmaier; Supervision, Ira Winkler, Elke Griesmaier and Anna Posod; Visualization, Elena Mayer, Eva Huber, Martina Urbanek and Anna Posod; Writing – original draft, Elena Mayer and Anna Posod; Writing – review & editing, Elena Mayer, Ira Winkler, Eva Huber, Martina Urbanek, Ursula Kiechl-Kohlendorfer, Elke Griesmaier and Anna Posod.

Funding: This research was funded by the "Fonds zur Förderung der wissenschaftlichen Forschung und des wissenschaftlichen Nachwuchses in Tirol (TWF)", grant number UNI-0404/1841.

Institutional Review Board Statement: The animal study protocol was approved by the Animal Welfare Body of the Medical University of Innsbruck, Austria and the Austrian Federal Ministry of Science, Research, and Economy (project number BMWFW-66.011/0003-WF/V/3b/2015, date of approval January 14th, 2015).

Informed Consent Statement: Not applicable.

Data Availability Statement: The original contributions presented in the study are included in the article; further inquiries can be directed to the corresponding author.

Acknowledgments: We sincerely thank all graduate students who participated in this project as part of their diploma thesis: Marie-Theres Lachinger and Bianca-Maria Vejnoska for performing animal experiments and obtaining somatometry data, Sandra Bergerweiß for quantification of activated microglia, Julia Saurer for quantification of cleaved Caspase-3-positive cells and Simon Gasser for literature research and review. Open Access Funding provided by the Medical University of Innsbruck.

Conflicts of Interest: The authors declare no conflicts of interest. The funders had no role in the design of the study; in the collection, analyses, or interpretation of data; in the writing of the manuscript; or in the decision to publish the results.

References

1. Hill MG, Reed KL, Brown RN. Perinatal asphyxia from the obstetric standpoint. Semin Fetal Neonatal Med 2021; 26(4):101259.
2. Juul SE, Ferriero DM. Pharmacologic neuroprotective strategies in neonatal brain injury. Clin Perinatol 2014; 41(1):119–31.
3. Golubnitschaja O, Yeghiazaryan K, Cebioglu M, Morelli M, Herrera-Marschitz M. Birth asphyxia as the major complication in newborns: moving towards improved individual outcomes by prediction, targeted prevention and tailored medical care. EPMA J 2011; 2(2):197–210.
4. Elsadek AE, FathyBarseem N, Suliman HA, Elshorbagy HH, Kamal NM, Talaat IM et al. Hepatic Injury in Neonates with Perinatal Asphyxia. Glob Pediatr Health 2021; 8:2333794X20987781.
5. UNICEF. Child Mortality Report 2023. United Nations Children's Fund; 2024 [cited October 4th of 2024]. Available from: URL: https://childmortality.org/wp-content/uploads/2024/03/UNIGME-2023-Child-Mortality-Report.pdf.
6. Villavicencio F, Perin J, Eilerts-Spinelli H, Yeung D, Prieto-Merino D, Hug L et al. Global, regional, and national causes of death in children and adolescents younger than 20 years: an open data portal with estimates for 2000-21. Lancet Glob Health 2024; 12(1):e16-e17.
7. Admasu FT, Melese BD, Amare TJ, Zewude EA, Denku CY, Dejenie TA. The magnitude of neonatal asphyxia and its associated factors among newborns in public hospitals of North Gondar Zone, Northwest Ethiopia: A cross-sectional study. PLoS One 2022; 17(3):e0264816.
8. Gillam-Krakauer M, Gowen Jr CW. StatPearls: Birth Asphyxia. Treasure Island (FL); 2024.
9. Lai M-C, Yang S-N. Perinatal hypoxic-ischemic encephalopathy. J Biomed Biotechnol 2011; 2011:609813.
10. Gopagondanahalli KR, Li J, Fahey MC, Hunt RW, Jenkin G, Miller SL et al. Preterm Hypoxic-Ischemic Encephalopathy. Front Pediatr 2016; 4:114.

 doi:10.20944/preprints202410.2113.v1

11. Cotten CM, Shankaran S. Hypothermia for hypoxic-ischemic encephalopathy. Expert Rev Obstet Gynecol 2010; 5(2):227–39.
12. Antonucci R, Porcella A, Pilloni MD. Perinatal asphyxia in the term newborn. Journal of Pediatric and Neonatal Individualized Medicine 2014; 3(2):e030269.
13. Distefano G, Praticò AD. Actualities on molecular pathogenesis and repairing processes of cerebral damage in perinatal hypoxic-ischemic encephalopathy. Ital J Pediatr 2010; 36:63.
14. Douglas-Escobar M, Weiss MD. Hypoxic-ischemic encephalopathy: a review for the clinician. JAMA Pediatr 2015; 169(4):397–403.
15. Greco P, Nencini G, Piva I, Scioscia M, Volta CA, Spadaro S et al. Pathophysiology of hypoxic-ischemic encephalopathy: a review of the past and a view on the future. Acta Neurol Belg 2020; 120(2):277–88.
16. Morales P, Bustamante D, Espina-Marchant P, Neira-Peña T, Gutiérrez-Hernández MA, Allende-Castro C et al. Pathophysiology of perinatal asphyxia: can we predict and improve individual outcomes? EPMA J 2011; 2(2):211–30.
17. Ruscher K, Wieloch T. The involvement of the sigma-1 receptor in neurodegeneration and neurorestoration. J Pharmacol Sci 2015; 127(1):30–5.
18. Griesmaier E, Posod A, Gross M, Neubauer V, Wegleiter K, Hermann M et al. Neuroprotective effects of the sigma-1 receptor ligand PRE-084 against excitotoxic perinatal brain injury in newborn mice. Experimental neurology 2012; 237(2):388–95.
19. Posod A, Pinzer K, Urbanek M, Wegleiter K, Keller M, Kiechl-Kohlendorfer U et al. The common antitussive agent dextromethorphan protects against hyperoxia-induced cell death in established in vivo and in vitro models of neonatal brain injury. Neuroscience 2014; 274:260–72.
20. Yang Z-J, Carter EL, Torbey MT, Martin LJ, Koehler RC. Sigma receptor ligand 4-phenyl-1-(4-phenylbutyl)-piperidine modulates neuronal nitric oxide synthase/postsynaptic density-95 coupling mechanisms and protects against neonatal ischemic degeneration of striatal neurons. Experimental neurology 2010; 221(1):166–74.
21. Ajmo CT, Vernon DOL, Collier L, Pennypacker KR, Cuevas J. Sigma receptor activation reduces infarct size at 24 hours after permanent middle cerebral artery occlusion in rats. Curr Neurovasc Res 2006; 3(2):89–98.
22. Takahashi H, Kirsch JR, Hashimoto K, London ED, Koehler RC, Traystman RJ. PPBP 4-phenyl-1-(4-phenylbutyl) piperidine decreases brain injury after transient focal ischemia in rats. Stroke 1996; 27(11):2120–3. Available from: URL: https://pubmed.ncbi.nlm.nih.gov/8898825/.
23. Quinn T, Greaves R, Badoer E, Walker D. DHEA in Prenatal and Postnatal Life: Implications for Brain and Behavior: Elsevier. Vitam Horm; 2018. (Vitamins and Hormones; vol 108).
24. Kroboth PD, Salek FS, Pittenger AL, Fabian TJ, Frye RF. DHEA and DHEA-S: a review. J Clin Pharmacol 1999; 39(4):327–48.
25. Rabe T, Ahrendt HJ, Albring C, Bachmann A, Bitzer, Blume-Peytavi U et al. Dehydroepiandrosterone and its Sulfate Joint: Statement by the German Society for Gynecological Endocrinology and Reproductive Medicine [DGGEF] and the German Professional Association of Gynecologists (BVF). Journal of Reproductive Medicine and Endocrinology 2015; (2 (4)):18–341.
26. Stárka L, Dušková M, Hill M. Dehydroepiandrosterone: a neuroactive steroid. The Journal of steroid biochemistry and molecular biology 2015; 145:254–60.
27. Yilmaz C, Karali K, Fodelianaki G, Gravanis A, Chavakis T, Charalampopoulos I et al. Neurosteroids as regulators of neuroinflammation. Front Neuroendocrinol 2019; 55:100788.
28. Lazaridis I, Charalampopoulos I, Alexaki V-I, Avlonitis N, Pediaditakis I, Efstathopoulos P et al. Neurosteroid dehydroepiandrosterone interacts with nerve growth factor (NGF) receptors, preventing neuronal apoptosis. PLoS Biol 2011; 9(4):e1001051.
29. Borowicz KK, Piskorska B, Banach M, Czuczwar SJ. Neuroprotective actions of neurosteroids. Front Endocrinol (Lausanne) 2011; 2:50.
30. Maninger N, Wolkowitz OM, Reus VI, Epel ES, Mellon SH. Neurobiological and neuropsychiatric effects of dehydroepiandrosterone (DHEA) and DHEA sulfate (DHEAS). Front Neuroendocrinol 2009; 30(1):65–91.
31. Kimonides VG, Khatibi NH, Svendsen CN, Sofroniew MV, Herbert J. Dehydroepiandrosterone (DHEA) and DHEA-sulfate (DHEAS) protect hippocampal neurons against excitatory amino acid-induced neurotoxicity. Proc Natl Acad Sci U S A 1998; 95(4):1852–7.
32. Cardounel A, Regelson W, Kalimi M. Dehydroepiandrosterone protects hippocampal neurons against neurotoxin-induced cell death: mechanism of action. Proceedings of the Society for Experimental Biology and Medicine. Society for Experimental Biology and Medicine (New York, N.Y.) 1999; 222(2):145–9. Available from: URL: https://pubmed.ncbi.nlm.nih.gov/10564538/.
33. Tao T, Liu G-J, Shi X, Zhou Y, Lu Y, Gao Y-Y et al. DHEA Attenuates Microglial Activation via Induction of JMJD3 in Experimental Subarachnoid Haemorrhage. J Neuroinflammation 2019; 16(1):243.
34. Li Z, Cui S, Zhang Z, Zhou R, Ge Y, Sokabe M et al. DHEA-neuroprotection and -neurotoxicity after transient cerebral ischemia in rats. J Cereb Blood Flow Metab 2009; 29(2):287–96.

 doi:10.20944/preprints202410.2113.v1

35. Lapchak PA, Chapman DF, Nunez SY, Zivin JA. Dehydroepiandrosterone sulfate is neuroprotective in a reversible spinal cord ischemia model: possible involvement of GABA(A) receptors. Stroke 2000; 31(8):1953-6; discussion 1957.
36. Li H, Klein G, Sun P, Buchan AM. Dehydroepiandrosterone (DHEA) reduces neuronal injury in a rat model of global cerebral ischemia. Brain Res 2001; 888(2):263–6.
37. Marx CE, Jarskog LF, Lauder JM, Gilmore JH, Lieberman JA, Morrow AL. Neurosteroid modulation of embryonic neuronal survival in vitro following anoxia. Brain Res 2000; 871(1):104–12.
38. Yabuki Y, Shinoda Y, Izumi H, Ikuno T, Shioda N, Fukunaga K. Dehydroepiandrosterone administration improves memory deficits following transient brain ischemia through sigma-1 receptor stimulation. Brain Res 2015; 1622:102–13.
39. Zhang L, Li Bs, Ma W, Barker JL, Chang YH, Zhao W et al. Dehydroepiandrosterone (DHEA) and its sulfated derivative (DHEAS) regulate apoptosis during neurogenesis by triggering the Akt signaling pathway in opposing ways. Brain Res Mol Brain Res 2002; 98(1-2):58–66.
40. Alexaki VI, Fodelianaki G, Neuwirth A, Mund C, Kourgiantaki A, Ieronimaki E et al. DHEA inhibits acute microglia-mediated inflammation through activation of the TrkA-Akt1/2-CREB-Jmjd3 pathway. Mol Psychiatry 2018; 23(6):1410–20.
41. Clark BJ, Prough RA, Klinge CM. Mechanisms of Action of Dehydroepiandrosterone. Vitam Horm 2018; 108:29–73.
42. Vannucci RC, Connor JR, Mauger DT, Palmer C, Smith MB, Towfighi J et al. Rat model of perinatal hypoxic-ischemic brain damage. J. Neurosci. Res. 1999; 55(2):158–63. Available from: URL: https://pubmed.ncbi.nlm.nih.gov/9972818/.
43. Hagberg H, Wilson MA, Matsushita H, Zhu C, Lange M, Gustavsson M et al. PARP-1 gene disruption in mice preferentially protects males from perinatal brain injury. J Neurochem 2004; 90(5):1068–75.
44. Dimauro I, Pearson T, Caporossi D, Jackson MJ. A simple protocol for the subcellular fractionation of skeletal muscle cells and tissue. BMC Res Notes 2012; 5:513.
45. Cox B, Emili A. Tissue subcellular fractionation and protein extraction for use in mass-spectrometry-based proteomics. Nat Protoc 2006; 1(4):1872–8.
46. Crowley LC, Waterhouse NJ. Detecting Cleaved Caspase-3 in Apoptotic Cells by Flow Cytometry. Cold Spring Harb Protoc 2016; 2016(11).
47. Tsang CK, Liu Y, Thomas J, Zhang Y, Zheng XFS. Superoxide dismutase 1 acts as a nuclear transcription factor to regulate oxidative stress resistance. Nat Commun 2014; 5:3446.
48. Ganguly U, Kaur U, Chakrabarti SS, Sharma P, Agrawal BK, Saso L et al. Oxidative Stress, Neuroinflammation, and NADPH Oxidase: Implications in the Pathogenesis and Treatment of Alzheimer's Disease. Oxid Med Cell Longev 2021; 2021:7086512.
49. Li Y, Zhao T, Li J, Xia M, Li Y, Wang X et al. Oxidative Stress and 4-hydroxy-2-nonenal (4-HNE): Implications in the Pathogenesis and Treatment of Aging-related Diseases. J Immunol Res 2022; 2022.
50. Valavanidis A, Vlachogianni T, Fiotakis C. 8-hydroxy-2' -deoxyguanosine (8-OHdG): A critical biomarker of oxidative stress and carcinogenesis. J Environ Sci Health C Environ Carcinog Ecotoxicol Rev 2009; 27(2):120–39.
51. Li Z, Zhou R, Cui S, Xie G, Cai W, Sokabe M et al. Dehydroepiandrosterone sulfate prevents ischemia-induced impairment of long-term potentiation in rat hippocampal CA1 by up-regulating tyrosine phosphorylation of NMDA receptor. Neuropharmacology 2006; 51(5):958–66.
52. Karishma KK, Herbert J. Dehydroepiandrosterone (DHEA) stimulates neurogenesis in the hippocampus of the rat, promotes survival of newly formed neurons and prevents corticosterone-induced suppression. Eur J Neurosci 2002; 16(3):445–53.
53. Yuan C, Gao J, Guo J, Bai L, Marshall C, Cai Z et al. Dimethyl sulfoxide damages mitochondrial integrity and membrane potential in cultured astrocytes. PLoS One 2014; 9(9):e107447.
54. Kurata K, Takebayashi M, Morinobu S, Yamawaki S. beta-estradiol, dehydroepiandrosterone, and dehydroepiandrosterone sulfate protect against N-methyl-D-aspartate-induced neurotoxicity in rat hippocampal neurons by different mechanisms. J Pharmacol Exp Ther 2004; 311(1):237–45.
55. Milman A, Zohar O, Maayan R, Weizman R, Pick CG. DHEAS repeated treatment improves cognitive and behavioral deficits after mild traumatic brain injury. Eur Neuropsychopharmacol 2008; 18(3):181–7.
56. Aragno M, Parola S, Brignardello E, Mauro A, Tamagno E, Manti R et al. Dehydroepiandrosterone prevents oxidative injury induced by transient ischemia/reperfusion in the brain of diabetic rats. Diabetes 2000; 49(11):1924–31.
57. Ferriero DM. Neonatal brain injury. N Engl J Med 2004; 351(19):1985–95.